

Competing Orders in a Nearly Antiferromagnetic Metal

Yoni Schattner,¹ Max H. Gerlach,² Simon Trebst,² and Erez Berg¹

¹*Department of Condensed Matter Physics, The Weizmann Institute of Science, Rehovot 76100, Israel*

²*Institute for Theoretical Physics, University of Cologne, 50937 Cologne, Germany*

(Received 11 January 2016; published 26 August 2016)

We study the onset of spin-density wave order in itinerant electron systems via a two-dimensional lattice model amenable to numerically exact, sign-problem-free determinantal quantum Monte Carlo simulations. The finite-temperature phase diagram of the model reveals a dome-shaped d -wave superconducting phase near the magnetic quantum phase transition. Above the critical superconducting temperature, an extended fluctuation regime manifests itself in the opening of a gap in the electronic density of states and an enhanced diamagnetic response. While charge density wave fluctuations are moderately enhanced in the proximity of the magnetic quantum phase transition, they remain short ranged. The striking similarity of our results to the phenomenology of many unconventional superconductors points a way to a microscopic understanding of such strongly coupled systems in a controlled manner.

DOI: 10.1103/PhysRevLett.117.097002

A common feature of many strongly correlated metals, such as the cuprates, the Fe-based superconductors, heavy-fermion compounds, and organic superconductors, is the close proximity of unconventional superconductivity (SC) and spin density wave (SDW) order in their phase diagrams. This suggests that there is a common, universal mechanism at work behind both phenomena [1–5]. In some of these systems, additional types of competing or coexisting orders appear upon suppressing the SDW order, such as nematic, charge-density wave (CDW), or possibly also pair density wave (PDW) order. Such a complex interplay between multiple types of electronic order, with comparable onset temperature scales, is a recurring theme in strongly correlated systems [6].

These findings call for a detailed understanding of the physics of metals on the verge of an SDW transition. Many studies have focused on the universal properties of an antiferromagnetic quantum critical point (QCP) in a metal [7–15]. However, due to the strongly coupled nature of the problem, no controlled solution has been available; all existing theoretical treatments involve uncontrolled approximations, whose validity is not obvious *a priori*. As a result, even the basic generic characteristics of metallic antiferromagnetic QCPs are still under debate.

Many studies have proposed that superconductivity is anomalously enhanced at the magnetic QCP [16–19]. The same antiferromagnetic interaction may enhance other subsidiary orders, such as CDW [18,20,21] or PDW [22,23]. Within a linearized “hot-spot” theory (which focuses on the vicinity of the points on the Fermi surface where fermions can scatter resonantly), a symmetry relating the SC and CDW orders emerges [18]. The strong fluctuations of the resulting multicomponent order parameter were proposed to be the origin of the “pseudogap” observed in the cuprates [20,24–26]; however, to what extent this

fluctuation regime plays a role beyond the linearized hot spot model has not been established. A deep minimum in the superfluid density at low temperature, seen in the iron-based SC $\text{BaFe}_2(\text{As}_{1-x}\text{P}_x)_2$ [27], has been proposed as a generic manifestation of the underlying antiferromagnetic QCP [28,29]. Other studies proposed a different mechanism for this behavior, unrelated to quantum criticality [30,31].

It is widely believed that the universal physics near the QCP depends only on the structure of the hot spots, and

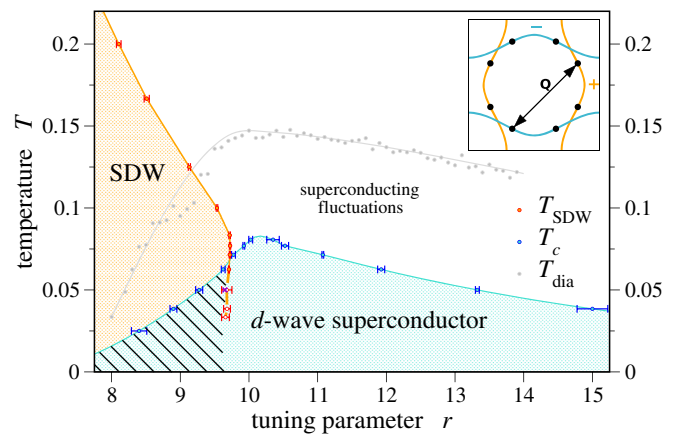


FIG. 1. Phase diagram of model (1) showing the transition temperature T_{SDW} to magnetic spin density wave (SDW) order, the superconducting T_c , and the onset of diamagnetism at T_{dia} . Solid lines indicate a Berezinskii-Kosterlitz-Thouless transition. The SDW transition inside the SC dome, marked by a dashed line, possibly is a weakly first-order transition (see the main text). The shaded region indicates the coexistence region between SDW and SC quasi-long-range orders. The inset shows the Fermi surface, with different colors indicating the sign of the superconducting order parameter. The hot spots and the SDW ordering wave vector \mathbf{Q} are marked.

not on the details of the Fermi surface away from them. In Ref. [32], a two-dimensional lattice model of a nearly antiferromagnetic metal, designed to capture this universal physics, has been introduced. At the same time, this model is amenable to sign-problem-free, determinantal quantum Monte Carlo (DQMC) simulations, thus allowing for a numerically exact solution. In this work, we numerically explore the phase diagram of a closely related model, as a function of temperature and a tuning parameter, shown in Fig. 1. This is the first time that such a phase diagram was obtained using a controlled, unbiased method. In addition, we systematically examine the role of subsidiary, emergent competing orders near the antiferromagnetic quantum phase transition (QPT). In the vicinity of the magnetic QPT we find a d -wave superconducting dome with a maximum T_c of the order of $E_F/30$, where E_F is the Fermi energy. In the superconducting state we find a region of coexistence with SDW order [33,35].

In addition to SC order, we have examined CDW and PDW ordering tendencies. While the CDW susceptibility shows a moderate enhancement in the vicinity of the QPT, there is no sign of a near degeneracy between the SC and CDW order parameters as the QPT is approached, suggesting that superconductivity is the only *generic* subsidiary order. Finally, the low-temperature superfluid density is found to vary smoothly, showing no pronounced minimum near the QPT.

Model.—Our lattice model consists of two flavors of spin- $\frac{1}{2}$ fermions, ψ_x and ψ_y , coupled to an SDW order parameter $\vec{\varphi}$ at wave vector $\mathbf{Q} = (\pi, \pi)$. The two flavor structure of the model guarantees the absence of the sign problem (see Refs. [32,34]). We assume that the SDW order parameter has an *easy-plane* character, and restrict the order parameter $\vec{\varphi}$ to lie in the XY plane. Using an $O(2)$ rather than $O(3)$ order parameter (as in Ref. [32]) gives rise to a *finite-temperature* SDW phase transition of Berezinskii-Kosterlitz-Thouless (BKT) character; it also allows for higher numerical efficiency.

The action is $S = S_F + S_\varphi = \int_0^\beta d\tau (L_F + L_\varphi)$ with

$$\begin{aligned} L_F &= \sum_{\substack{i,j,s \\ \alpha=x,y}} \psi_{ais}^\dagger [(\partial_\tau - \mu)\delta_{ij} - t_{aij}] \psi_{ajs} \\ &\quad + \lambda \sum_{i,s,s'} e^{i\mathbf{Q}\cdot\mathbf{r}_i} [\vec{s} \cdot \vec{\varphi}_i]_{ss'} \psi_{xis}^\dagger \psi_{yis'} + \text{H.c.}, \\ L_\varphi &= \frac{1}{2} \sum_i \frac{1}{c^2} \left(\frac{d\vec{\varphi}_i}{d\tau} \right)^2 + \frac{1}{2} \sum_{\langle i,j \rangle} (\vec{\varphi}_i - \vec{\varphi}_j)^2 \\ &\quad + \sum_i \left[\frac{r}{2} \vec{\varphi}_i^2 + \frac{u}{4} (\vec{\varphi}_i^2)^2 \right]. \end{aligned} \quad (1)$$

Here i, j label the sites of a square lattice, $\alpha = x, y$ are flavor indices, $s, s' = \uparrow, \downarrow$ are spin indices, and \vec{s} are Pauli matrices. τ denotes imaginary time and $\beta = 1/T$ the inverse temperature. The hopping amplitudes for the ψ_x -fermions

along the horizontal and vertical lattice directions are $t_{x,h} = 1$ and $t_{x,v} = 0.5$, respectively, while for the ψ_y fermions $t_{y,h} = 0.5$ and $t_{y,v} = 1$. (The inset of Fig. 1 shows the Fermi surfaces.) r is a tuning parameter used to tune the system to the vicinity of an SDW instability. Physically, r can be thought of as doping or pressure. We set the chemical potential to $\mu = 0.5$, the quartic coupling to $u = 1$, the Yukawa coupling to $\lambda = 3$, and the bare bosonic velocity to $c = 2$.

Numerical simulations.— We study model (1) by extensive DQMC [36–39] simulations. Simulations were performed with a single flux quantum threaded through the system, which dramatically improves the approach to the thermodynamic limit for metallic systems [40,41]. For details of this procedure and other technical aspects of the DQMC simulations and data analysis we refer to the Supplemental Material [34]. We report results up to linear extent $L = 14$ and temperatures down to $T = 0.025$.

Phase diagram.— Our main finding is the phase diagram of model (1) as shown in Fig. 1. The system displays a quasi-long-range ordered SDW phase, whose transition temperature, T_{SDW} , decreases upon increasing r . In the vicinity of the magnetic QPT where T_{SDW} collapses to zero, we find a region with quasi-long-range d -wave superconducting order. The superconducting T_c traces an asymmetric domelike shape as a function of r and reaches a maximum of $T_c^{\text{max}} \approx 0.08$ at $r_{\text{opt}} \approx 10.2$. Between the two distinct phases we find a region where both types of quasi-long-range order coexist.

At sufficiently high temperatures, the antiferromagnetic transition is consistent with BKT character. In this regime the SDW susceptibility $\chi = \int d\tau \sum_i \langle \vec{\varphi}_i(\tau) \cdot \vec{\varphi}_0(0) \rangle$ for different system sizes nicely follows the expected scaling behavior $\chi \propto L^{2-\eta}$, with η changing continuously as a function of r and T [34]. We identify T_{SDW} as the point where we observe the BKT value $\eta = 1/4$. At low temperatures, $T \lesssim 0.05$ (i.e., within the SC region), the situation is less clear with the numerical data starting to systematically deviate from this scaling behavior. In fact, there are indications that the transition may become weakly first order at sufficiently low T ; see the discussion in the Supplemental Material [34].

The SC transition is identified as the point where the superfluid density obtains the universal BKT value $2T/\pi$ [42,43], and is always consistent with BKT behavior. The nature of the superconducting state is revealed in the uniform pairing susceptibilities $P_\eta(\mathbf{q} = \mathbf{0})$, where $P_\eta(\mathbf{q}) = \int d\tau \langle \Delta_\eta^\dagger(\mathbf{q}, \tau) \Delta_\eta(\mathbf{q}, 0) \rangle$, and $\Delta_\eta(\mathbf{r}_i) = 2(\psi_{xi\uparrow}^\dagger \psi_{xi\downarrow}^\dagger + \eta \psi_{yi\uparrow}^\dagger \psi_{yi\downarrow}^\dagger)$ with $\eta = \pm 1$. Under a $\pi/2$ rotation, associated with a rotation matrix $R_{\pi/2}$, we have $\Delta_\eta(\mathbf{r}) \rightarrow \eta \Delta_\eta(R_{\pi/2}\mathbf{r})$; i.e., Δ_- has a d -wave (B_{1g}) character. At low temperatures $P_-(\mathbf{q} = \mathbf{0})$, shown in Fig. 2(b), is found to increase rapidly with system size, indicating that the SC phase has d -wave symmetry in the thermodynamic limit. In contrast, the

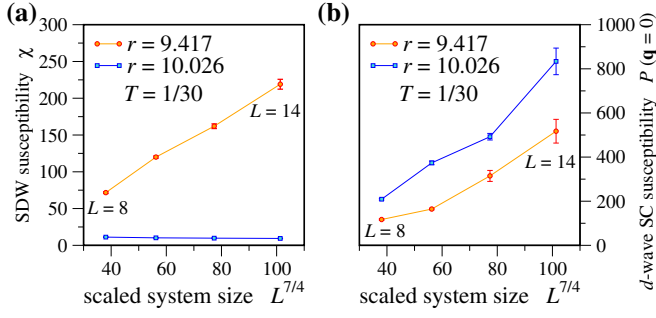


FIG. 2. (a) SDW susceptibility χ and (b) d -wave superconducting susceptibility $P_-(\mathbf{q} = 0)$ at $T = 1/30$ in the region of phase coexistence at $r = 9.417$ and in the nonmagnetic superconducting phase at $r = 10.026$.

s -wave pairing susceptibility $P_+(\mathbf{q} = 0)$ is found to be much smaller and system size independent [34].

In the shaded region of Fig. 1, we find that both the SDW and the SC susceptibilities grow faster than $\sim L^{7/4}$ with the system size; see Fig. 2. This indicates that in this region, the two quasi-long-range orders coexist.

A striking feature seen in the phase diagram is the kinklike change of slope of the SDW and SC phase boundaries in the r - T plane upon meeting each other. A related “back bending” is also apparent in the magnetic susceptibility over a wide range of r as shown in Fig. 3(a). Tracking the SDW susceptibility for fixed r , as shown in Fig. 3(b), one finds nonmonotonic behavior with a maximum seen near T_c . Such behavior, generally expected for order parameters interacting through a repulsive quartic term [44], has been predicted to arise from the competition between the two order parameters [45], and has been observed in certain unconventional superconductors, such as $\text{Ba}_{1-x}\text{Co}_x\text{Fe}_2\text{As}_2$ [46].

In a finite range of temperatures above T_c , the orbital magnetic susceptibility is diamagnetic in sign (unlike the high temperature susceptibility, which is paramagnetic in our model), and its magnitude rapidly grows with

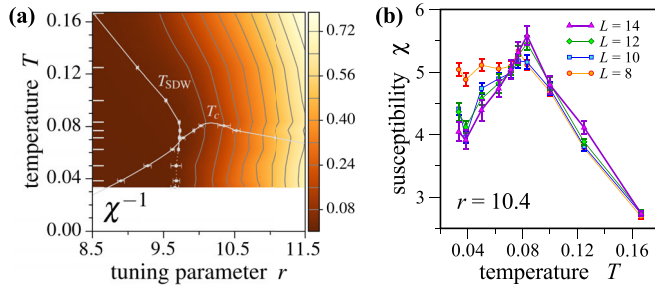


FIG. 3. (a) Inverse magnetic susceptibility across the phase diagram with the gray lines indicating contour lines. We show data for $L = 14$ at those temperatures indicated by ticks on the left inside of the plot and interpolate linearly between them. (b) Magnetic susceptibility near the maximum of the superconducting dome as a function of temperature for different system sizes.

decreasing temperature. We identify this behavior as a signature of substantial finite-range superconducting fluctuations. The temperature where the orbital susceptibility changes sign, denoted by T_{dia} , is indicated by the gray dots in Fig. 1. Over much of the phase diagram, T_{dia} roughly follows the shape of the superconducting dome, i.e., $T_{\text{dia}} \propto T_c$. Another manifestation of finite-range superconducting fluctuations is the opening of a gap in the single-particle density of states (DOS) $N(\omega, T)$ above T_c . While we cannot access $N(\omega, T)$ directly without performing an analytical continuation, we can use the relation [47] $\tilde{N}(T) = (1/\pi L^2 T) \text{Tr} G(\tau = \beta/2) = \int_{-\infty}^{\infty} \{ [d\omega] / [2\pi T \cosh(\beta\omega/2)] \} N(\omega, T)$, to extract information about the low-energy DOS. Here, G is the imaginary time single-particle Green’s function. Note that $\tilde{N}(T \rightarrow 0) = N(\omega = 0, T = 0)$. This integrated DOS $\tilde{N}(T)$ is shown in Fig. 4. In the SDW state, the behavior is consistent with a partial gapping of the Fermi surface, which, due to magnetic fluctuations, commences slightly above the magnetic ordering temperature T_{SDW} [see panels (a) and (b)]. A similar reduction of $\tilde{N}(T)$, which we associate with superconducting fluctuations, sets in above the superconducting T_c , in correlation with T_{dia} . See panels (b), (c), and (d). Extrapolating $\tilde{N}(T)$ to $T = 0$ indicates that the superconducting state is fully gapped [48].

CDW and PDW susceptibilities.—We now turn to examine susceptibilities of various density-wave orders. We define the CDW susceptibility $C_\eta(\mathbf{q}) = \int d\tau \langle n_\eta^\dagger(\mathbf{q}, \tau) n_\eta(\mathbf{q}, 0) \rangle$, where $n_\eta(\mathbf{r}_i) = \sum_{s=\uparrow, \downarrow} (\psi_{xis}^\dagger \psi_{xis} + \eta \psi_{yis}^\dagger \psi_{yis})$ and $\eta = \pm 1$. Note that similarly to Δ_- , n_- has a d -wave (B_{1g}) character.

In Fig. 5 we show the momentum dependence of C_- and P_- . P_- is strongly peaked at $\mathbf{q} = 0$ and does not display much structure at other momenta, indicating that there is no noticeable tendency towards PDW order. $P_+(\mathbf{q} = 0)$

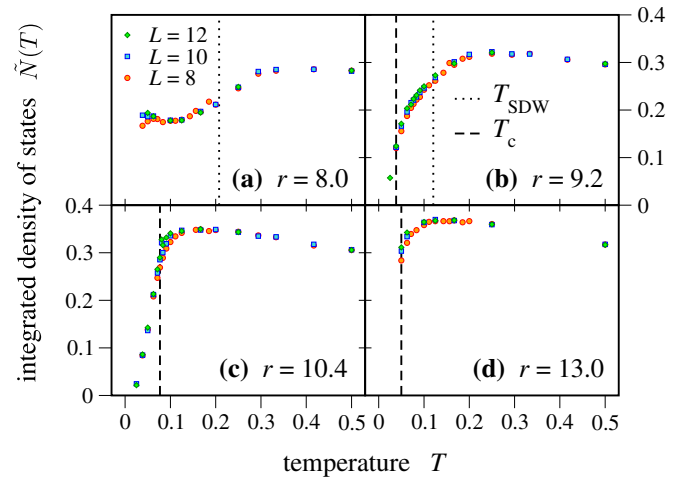


FIG. 4. The integrated density of states $\tilde{N}(T)$, as defined in the text, versus temperature for various values of the tuning parameter r . The dashed (dotted) lines indicate the location of the SC (SDW) transition temperatures, respectively.

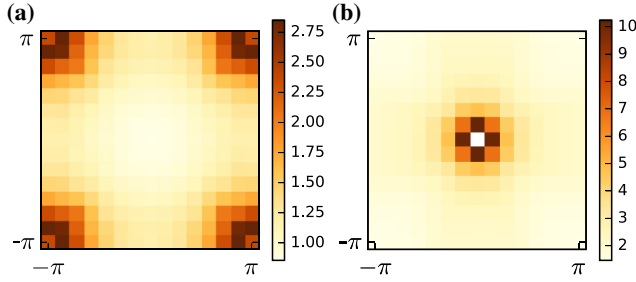


FIG. 5. (a) d -wave CDW and (b) d -wave PDW susceptibilities, as defined in the text, across the Brillouin zone. Shown here is data for $L = 14$, $T = 0.083$, and $r = 10.4$. The data point $P_-(\mathbf{q} = \mathbf{0})$ (i.e., the uniform superconducting susceptibility) has been excluded from the data (white square).

(not shown [34]) is significantly smaller in amplitude, and also shows no structure at finite momenta. C_- is maximal in the vicinity of (but away from) $\mathbf{q} = (\pi, \pi)$. $C_+(\mathbf{q})$ (not shown [34]) is qualitatively similar to $C_-(\mathbf{q})$, although its maximal value is approximately 3 times lower. We find that several bond-centered charge orders (not shown [34]) do not exhibit strong temperature or size dependence.

Focusing on C_- , we show its momentum dependence along the high-symmetry cut $\mathbf{q} = (\pi, q_y)$ in Fig. 6(a). The data taken from different system sizes collapse onto a single curve, suggesting that the CDW correlation length is sufficiently short such that results are representative of the thermodynamic limit. The temperature dependence of C_- at the CDW wave vector $\mathbf{q}_{\max} = (\pi, q_{\max})$, where it is maximal ($q_{\max} \approx 0.83\pi$) is shown in Fig. 6(b) for different values of r on either side of the magnetic QPT. We find that $C_-(\mathbf{q}_{\max}, T)$ is maximal at a temperature close to $\max(T_c, T_{\text{SDW}})$. This can be understood as a consequence of the reduction in the DOS due to the SC or SDW order. Across the entire phase diagram, the maximal CDW susceptibility is obtained at $r \approx r_{\text{opt}}$, close to the SDW QPT. Note, however, that near T_c the d -wave pairing susceptibility P_- is at least an order of magnitude larger than the CDW susceptibility.

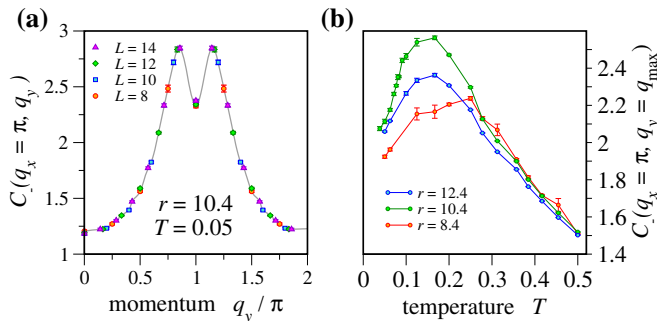


FIG. 6. (a) The d -wave CDW susceptibility versus momentum along the high-symmetry cut $\mathbf{q} = (\pi, q_y)$ for various system sizes. The solid line is a guide to the eye. (b) Temperature dependence of the CDW susceptibility at the optimal q (taken at $L = 12$), for multiple values of r .

Superfluid density.— Finally, we examine the low-temperature superfluid density across the phase diagram, proposed to exhibit a sharp minimum at a magnetic QCP [29]. Figure 7 shows the finite-size superfluid density $\rho_s(L)$ [34] along a cut through the superconducting dome at a fixed temperature, $T = 0.025$. Notably, we find that inside the SC dome $\rho_s(L)$ is only weakly r dependent, with no apparent minimum anywhere in the superconducting phase. This is consistent with predictions of a field theoretical analysis [30] and with the observed behavior in $\text{Ba}_{1-x}\text{Co}_x\text{Fe}_2\text{As}_2$ [49], and suggests that the sharp minimum observed in $\text{BaFe}_2(\text{As}_{1-x}\text{P}_x)_2$ may be of a different origin (see, e.g., Ref. [31]).

Discussion.—The striking similarity between the phase diagram of our model and the phase diagrams of many unconventional superconductors, such as the iron-based SC, electron-doped cuprates or organic SC, strongly suggests that much of the essential physics in these systems is indeed captured within our model, as has been long anticipated [5]. This encouraging result calls for further investigations of extensions of this basic model, designed to capture more material-specific features. First steps in this direction have been taken recently [50,51].

Since models similar to the one studied here are frequently invoked to describe the phenomenology of the hole-doped cuprate superconductors, it is interesting to contrast the behavior seen in our model to that of the cuprates. Our model exhibits a gap in the single particle spectrum that precedes the phase transitions into the SC and SDW phases, as has been predicted for a nearly antiferromagnetic metal [52]. However, the onset temperature of the gap roughly follows the ordering temperature, and is never larger than about twice the corresponding transition temperature. In this sense, our results are different from the pseudogap phase of the cuprates. Our model also displays diamagnetic fluctuations with an onset temperature proportional to, and significantly above, T_c . Similar phenomena have been observed in the cuprates [53,54].

In addition to unconventional superconductivity, our model exhibits an enhancement of CDW fluctuations with

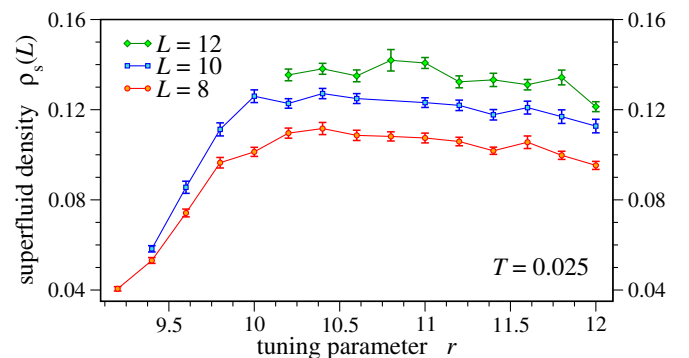


FIG. 7. The finite-size superfluid density $\rho_s(L)$ within the superconducting phase versus r at $T = 0.025$.

a d -wave form factor. However, the CDW susceptibility is only moderately enhanced compared to the expectation based on the noninteracting band structure. The quasi-one-dimensional character of the dispersion of each fermion flavor enhances the CDW susceptibility, although at a nonzero chemical potential there is no “perfect nesting” [34]. It seems that the interaction mediated by spin fluctuations is not sufficient, by itself, to promote strong CDW fluctuations. This is consistent with the conclusions of Refs. [55–58] that additional, nonmagnetic interactions are needed to stabilize a CDW phase.

Finally, since in our model the magnetic QPT occurs inside a superconducting phase, our results do not have a direct bearing on the question of metallic SDW quantum criticality. In addition, we found some indications that at low temperatures, the SDW transition may become weakly first order. Nevertheless, since $T_c \ll E_F$, one can still expect to see a substantial crossover regime above T_c , where the physics is dominated by an underlying “avoided” QCP. Indeed, we have preliminary indications that above T_c , the dynamic SDW susceptibility exhibits Landau damping [59]. Whether this regime is characterized by a breakdown of Fermi liquid behavior, as observed in many unconventional superconductors, remains to be seen.

We thank D. Chowdhury, R. Fernandes, E. Fradkin, S. Kivelson, S. Sachdev, D. J. Scalapino, and C. Varma for their useful comments on this Letter. The numerical simulations were performed on the CHEOPS cluster at RRZK Cologne, the JUROPA/JURECA clusters at the Forschungszentrum Jülich, and the ATLAS cluster at the Weizmann Institute. Y. S. and E. B. were supported by the Israel Science Foundation under Grant No. 1291/12, by the US-Israel BSF under Grant No. 2014209, and by a Marie Curie reintegration grant. E. B. was supported by an Alon fellowship. M. G. thanks the Bonn-Cologne Graduate School of Physics and Astronomy (BCGS) for support.

Y. S. and M. H. G. contributed equally to this work.

Note added.—While we were preparing this manuscript, Ref. [60] appeared, where a closely related model with O(3) symmetry was studied. Our results are qualitatively similar to those of Ref. [60] where they overlap.

-
- [1] D. Scalapino, E. Loh Jr., and J. Hirsch, d -wave pairing near a spin-density-wave instability, *Phys. Rev. B* **34**, 8190 (1986).
 [2] K. Miyake, S. Schmitt-Rink, and C. M. Varma, Spin-fluctuation-mediated even-parity pairing in heavy-fermion superconductors, *Phys. Rev. B* **34**, 6554 (1986).
 [3] N. E. Bickers, D. J. Scalapino, and S. R. White, Conserving Approximations for Strongly Correlated Electron Systems: Bethe-Salpeter Equation and Dynamics for the Two-Dimensional Hubbard Model, *Phys. Rev. Lett.* **62**, 961 (1989).

- [4] P. Monthoux, A. Balatsky, and D. Pines, Toward a Theory of High-Temperature Superconductivity in the Antiferromagnetically Correlated Cuprate Oxides, *Phys. Rev. Lett.* **67**, 3448 (1991).
 [5] For a recent review, see D. J. Scalapino, A common thread: The pairing interaction for unconventional superconductors, *Rev. Mod. Phys.* **84**, 1383 (2012).
 [6] E. Fradkin, S. A. Kivelson, and J. M. Tranquada, Colloquium: Theory of intertwined orders in high temperature superconductors, *Rev. Mod. Phys.* **87**, 457 (2015).
 [7] J. A. Hertz, Quantum critical phenomena, *Phys. Rev. B* **14**, 1165 (1976).
 [8] A. J. Millis, Effect of a nonzero temperature on quantum critical points in itinerant fermion systems, *Phys. Rev. B* **48**, 7183 (1993).
 [9] A. Abanov and A. Chubukov, Spin-Fermion Model near the Quantum Critical Point: One-Loop Renormalization Group Results, *Phys. Rev. Lett.* **84**, 5608 (2000).
 [10] A. Abanov, A. Chubukov, and J. Schmalian, Quantum-critical theory of the spin-fermion model and its application to cuprates: Normal state analysis, *Adv. Phys.* **52**, 119 (2003).
 [11] A. Abanov and A. Chubukov, Anomalous Scaling at the Quantum Critical Point in Itinerant Antiferromagnets, *Phys. Rev. Lett.* **93**, 255702 (2004).
 [12] H. V. Löhneysen, A. Rosch, M. Vojta, and P. Wölfle, Fermi-liquid instabilities at magnetic quantum phase transitions, *Rev. Mod. Phys.* **79**, 1015 (2007).
 [13] M. Metlitski and S. Sachdev, Quantum phase transitions of metals in two spatial dimensions. II. Spin density wave order, *Phys. Rev. B* **82**, 075128 (2010).
 [14] C. M. Varma, Quantum Criticality in Quasi-Two-Dimensional Itinerant Antiferromagnets, *Phys. Rev. Lett.* **115**, 186405 (2015).
 [15] C. M. Varma, L. Zhu, and A. Schröder, Quantum critical response function in quasi-two-dimensional itinerant antiferromagnets, *Phys. Rev. B* **92**, 155150 (2015).
 [16] A. Abanov, A. V. Chubukov, and A. M. Finkel'stein, Coherent vs. incoherent pairing in 2D systems near magnetic instability, *Europhys. Lett.* **54**, 488 (2001).
 [17] A. Abanov, A. Chubukov, and M. Norman, Gap anisotropy and universal pairing scale in a spin-fluctuation model of cuprate superconductors, *Phys. Rev. B* **78**, 220507 (2008).
 [18] M. A. Metlitski and S. Sachdev, Instabilities near the onset of spin density wave order in metals, *New J. Phys.* **12**, 105007 (2010).
 [19] Y. Wang and A. V. Chubukov, Superconductivity at the Onset of Spin-Density-Wave Order in a Metal, *Phys. Rev. Lett.* **110**, 127001 (2013).
 [20] K. B. Efetov, H. Meier, and C. Pepin, Pseudogap state near a quantum critical point, *Nat. Phys.* **9**, 442 (2013).
 [21] Y. Wang and A. Chubukov, Charge-density-wave order with momentum $(2Q, 0)$ and $(0, 2Q)$ within the spin-fermion model: Continuous and discrete symmetry breaking, preemptive composite order, and relation to pseudogap in hole-doped cuprates, *Phys. Rev. B* **90**, 035149 (2014).
 [22] Y. Wang, D. F. Agterberg, and A. Chubukov, Interplay between pair- and charge-density-wave orders in underdoped cuprates, *Phys. Rev. B* **91**, 115103 (2015).
 [23] Y. Wang, D. F. Agterberg, and A. Chubukov, Coexistence of Charge-Density-Wave and Pair-Density-Wave Orders in Underdoped Cuprates, *Phys. Rev. Lett.* **114**, 197001 (2015).

- [24] L. E. Hayward, D. G. Hawthorn, R. G. Melko, and S. Sachdev, Angular fluctuations of a multicomponent order describe the pseudogap of $\text{YBa}_2\text{Cu}_3\text{O}_{6+x}$, *Science* **343**, 1336 (2014).
- [25] H. Meier, C. Pépin, M. Einenkel, and K. B. Efetov, Cascade of phase transitions in the vicinity of a quantum critical point, *Phys. Rev. B* **89**, 195115 (2014).
- [26] C. Pépin, V. S. de Carvalho, T. Kloss, and X. Montiel, Pseudogap, charge order, and pairing density wave at the hot spots in cuprate superconductors, *Phys. Rev. B* **90**, 195207 (2014).
- [27] K. Hashimoto, K. Cho, T. Shibauchi, S. Kasahara, Y. Mizukami, R. Katsumata, Y. Tsuruhara, T. Terashima, H. Ikeda, M. A. Tanatar, H. Kitano, N. Salovich, R. W. Giannetta, P. Walmsley, A. Carrington, R. Prozorov, and Y. Matsuda, A sharp peak of the zero-temperature penetration depth at optimal composition in $\text{BaFe}_2(\text{As}_{1-x}\text{P}_x)_2$, *Science* **336**, 1554 (2012).
- [28] A. Levchenko, M. Vavilov, M. Khodas, and A. Chubukov, Enhancement of the London Penetration Depth in Pnictides at the Onset of Spin-Density-Wave Order under Superconducting Dome, *Phys. Rev. Lett.* **110**, 177003 (2013).
- [29] T. Shibauchi, A. Carrington, and Y. Matsuda, A quantum critical point lying beneath the superconducting dome in iron pnictides, *Annu. Rev. Condens. Matter Phys.* **5**, 113 (2014).
- [30] D. Chowdhury, B. Swingle, E. Berg, and S. Sachdev, Singularity of the London Penetration Depth at Quantum Critical Points in Superconductors, *Phys. Rev. Lett.* **111**, 157004 (2013).
- [31] D. Chowdhury, J. Orenstein, S. Sachdev, and T. Senthil, Phase transition beneath the superconducting dome in $\text{BaFe}_2(\text{As}_{1-x}\text{P}_x)_2$, *Phys. Rev. B* **92**, 081113(R) (2015).
- [32] E. Berg, M. A. Metlitski, and S. Sachdev, Sign-problem-free quantum Monte Carlo of the onset of antiferromagnetism in metals, *Science* **338**, 1606 (2012).
- [33] Our estimate for the magnetic phase boundary at low temperatures (within the superconducting phase) are less accurate than the estimate of the phase boundary at higher temperatures, since finite size effects are more pronounced in the low temperature regime (see Supplemental Material [34]).
- [34] See Supplemental Material at <http://link.aps.org/supplemental/10.1103/PhysRevLett.117.097002> for a detailed discussion of the numerical approach, the procedure for locating the magnetic and superconducting transitions, the calculation of the diamagnetic response, and additional data for CDW and PDW susceptibilities.
- [35] The fact that unconventional SC order is compatible with a coexistence region with SDW order was pointed out in R. M. Fernandes and J. Schmalian, Competing order and nature of the pairing state in the iron pnictides, *Phys. Rev. B* **82**, 014521 (2010).
- [36] R. Blankenbecler, D. J. Scalapino, and R. L. Sugar, Monte Carlo calculations of coupled boson-fermion systems. I, *Phys. Rev. D* **24**, 2278 (1981).
- [37] S. R. White, D. J. Scalapino, R. L. Sugar, E. Y. Loh, J. E. Gubernatis, and R. T. Scalettar, Numerical study of the two-dimensional Hubbard model, *Phys. Rev. B* **40**, 506 (1989).
- [38] E. Loh Jr. and J. E. Gubernatis, Stable numerical simulations of models of interacting electrons in condensed-matter physics, in *Electron. Phase Transitions*, Modern Problems in Condensed Matter Sciences, Vol. 10, edited by W. Hanke and Y. Kopayev (North Holland, Amsterdam, 1992), Chap. 4.
- [39] F. Assaad and H. Evertz, World-line and determinantal quantum Monte Carlo methods for spins, phonons and electrons, in *Comput. Many-Particle Phys.*, Lect. Notes Phys., Vol. 739, edited by H. Fehske, R. Schneider, and A. Weiße (Springer, New York, 2008), p. 277.
- [40] F. F. Assaad, Depleted Kondo lattices: Quantum Monte Carlo and mean-field calculations, *Phys. Rev. B* **65**, 115104 (2002).
- [41] Y. Schattner, S. Lederer, S. A. Kivelson, and E. Berg, Ising nematic quantum critical point in a metal: A Monte Carlo study, [arXiv:1511.03282](https://arxiv.org/abs/1511.03282).
- [42] T. Paiva, R. R. dos Santos, R. T. Scalettar, and P. J. H. Denteneer, Critical temperature for the two-dimensional attractive Hubbard model, *Phys. Rev. B* **69**, 184501 (2004).
- [43] D. J. Scalapino, S. R. White, and S. Zhang, Insulator, metal, or superconductor: The criteria, *Phys. Rev. B* **47**, 7995 (1993).
- [44] P. M. Chaikin and T. C. Lubensky, *Principles of Condensed Matter Physics*, Vol. 1 (Cambridge University Press, Cambridge, 2000).
- [45] E. G. Moon and S. Sachdev, Competition between spin density wave order and superconductivity in the underdoped cuprates, *Phys. Rev. B* **80**, 035117 (2009).
- [46] N. Ni, A. Thaler, J. Q. Yan, A. Kracher, E. Colombier, S. L. Bud'Ko, P. C. Canfield, and S. T. Hannahs, Temperature versus doping phase diagrams for $\text{Ba}(\text{Fe}_{1-x}\text{TM}_x)_2\text{As}_2$ (TM = Ni, Cu, Co) single crystals, *Phys. Rev. B* **82**, 024519 (2010).
- [47] N. Trivedi and M. Randeria, Deviations from Fermi-Liquid Behavior Above T_c in 2D Short Coherence Length Superconductors, *Phys. Rev. Lett.* **75**, 312 (1995).
- [48] Because of the two-band structure of our model, a d -wave SC order parameter can be nodeless (see inset of Fig. 1).
- [49] L. Luan, T. M. Lippman, C. W. Hicks, J. A. Bert, O. M. Auslaender, J.-H. Chu, J. G. Analytis, I. R. Fisher, and K. A. Moler, Local Measurement of the Superfluid Density in the Pnictide Superconductor $\text{Ba}(\text{Fe}_{1-x}\text{Co}_x)_2\text{As}_2$ across the Superconducting Dome, *Phys. Rev. Lett.* **106**, 067001 (2011).
- [50] Z.-X. Li, F. Wang, H. Yao, and D.-H. Lee, What makes the T_c of monolayer FeSe on SrTiO_3 so high: a sign-problem-free quantum Monte Carlo study, *Sci. Bull.* **61**, 925 (2016).
- [51] P. T. Dumitrescu, M. Serbyn, R. T. Scalettar, and A. Vishwanath, Superconductivity and Nematic Fluctuations in a model of FeSe monolayers: A Determinant Quantum Monte Carlo Study, [arXiv:1512.08523](https://arxiv.org/abs/1512.08523).
- [52] J. Schmalian, D. Pines, and B. Stojković, Microscopic theory of weak pseudogap behavior in the underdoped cuprate superconductors: General theory and quasiparticle properties, *Phys. Rev. B* **60**, 667 (1999).
- [53] L. Li, Y. Wang, M. Naughton, S. Ono, Y. Ando, and N. Ong, Strongly nonlinear magnetization above T_c in $\text{Bi}_2\text{Sr}_2\text{CaCu}_2\text{O}_{8+\delta}$, *Europhys. Lett.* **72**, 451 (2005).
- [54] L. Li, Y. Wang, S. Komiya, S. Ono, Y. Ando, G. D. Gu, and N. P. Ong, Diamagnetism and Cooper pairing above T_c in cuprates, *Phys. Rev. B* **81**, 054510 (2010).

- [55] S. Sachdev and R. La Placa, Bond order in Two-Dimensional Metals with Antiferromagnetic Exchange Interactions, *Phys. Rev. Lett.* **111**, 027202 (2013).
- [56] J.D. Sau and S. Sachdev, Mean-field theory of competing orders in metals with antiferromagnetic exchange interactions, *Phys. Rev. B* **89**, 075129 (2014).
- [57] A. Allais, J. Bauer, and S. Sachdev, Density wave instabilities in a correlated two-dimensional metal, *Phys. Rev. B* **90**, 155114 (2014).
- [58] V. Mishra and M.R. Norman, Strong coupling critique of spin fluctuation driven charge order in underdoped cuprates, *Phys. Rev. B* **92**, 060507 (2015).
- [59] M. Gerlach, Y. Schattner, E. Berg, and S. Trebst (to be published).
- [60] Z.-X. Li, F. Wang, H. Yao, and D.-H. Lee, The nature of effective interaction in cuprate superconductors: a sign-problem-free quantum Monte-Carlo study (to be published).